+

EFFECT OF DESIGN CONDITIONS ON REHEAT GAS TURBINE COMBINED CYCLE POWER USING TRANSCRITICAL CARBON DIOXIDE AND AMMONIA WATER MIXTURE

Jyoti Singh[1], Dr. Mayank Maheshwari[2], Dr. Apurva Anand[3]

Article History: Received: 20.03.2023 **Revised:** 06.06.2023 **Accepted:** 12.07.2023

Abstract:

It is continually being researched and improved upon how to make thermodynamic power cycles as efficient as the Carnot cycle. Various strategies that have been tested and are performing well are included in these efforts to improve the thermal efficiency of the cycle. Due to their high efficiency, coupled cycles have become a popular option for power cycles. However, there is still room for improvement by making more changes to the thermodynamic cycle's thermal efficiency. Based on the first and second laws of thermodynamics, the present study examines the impact of ambient temperature and design parameters such as cycle pressure ratio and turbine inlet temperature in a combined cycle using transcritical carbon dioxide, and a binary mixture of ammonia and water. The result of the energy and exergy analysis of considered combined cycle using ammonia water mixture show that when maximum work output is obtained then thefirst law efficiency and second law efficiency are at value of 62.01% and 60.27% respectively. This lesser value of second law efficiency opens opportunities for removing sources of inefficiencies to make combined cycles much more efficient.

Keyword: Reheat Gas Turbine Cycle, Transcritical carbon dioxide, Concentration of Ammonia, Heat recovery generator.

[1]Phd Scholar, BBD University, Lucknow
[2]Associate Professor, Allenhouse Institute of Technology Kanpur
[3]Professor, MPEC, Kanpur

DOI: 10.31838/ecb/2023.12.3.184

1. Introduction

In view of natural aspiration, the gas turbine power plants/combined cycle based power plants are being affected by the atmospheric conditions. The installation of various thermodynamic elements for conditioning of admitting air, ultimately affects the performance of power cycle which may be in terms of power or efficiency or economy.[1] Chen et.al presents Transcritical CO2 has advantages over conventional systems using other working fluids for low grade heat source recovery because it transfers heat more effectively than other pure working fluids. The analysis uses a straightforward carbon dioxide transcritical power system with an internal heat exchanger (IHX), and the system performance is contrasted with a straightforward organic Rankin cycle (ORC). It has been discovered that there is an ideal gas heater pressure for a specific cycle working state, and that the ideal pressure value decreases as the heat source temperature decreases. Under specific cycle conditions, adding an internal heat exchanger can increase efficiency by 50%.
[2] Aqul et.al. presents It can be used for dry cooling in arid climates to dope CO2 (with non-organic dopant like TiCl4, NOD, or C6F6) with various materials to raise the critical temperature and improve thermodynamic cycle performance. TiCl4 has the highest efficiency, up to 49.4%, but the specific work is reduced. Due to the presence of all three dopants, the fluid's density rises at the turbine's inlet, and the sound speed falls there. Dopants heavier than CO2 are required to modify the CO2 working fluid and raise its critical temperature in order to use it in condensing cycles for CSP applications.
[3] Wang et.al. presents , When the evaporator and absorber are at 140 0C/ 4000 kPa and 25 0C/ 800 kPa, respectively, and the diaphragm pump is used to pump the liquid from the absorber to the evaporator, the net work and thermal efficiency are 10.68 kW and 9.9%, respectively. When compared to the conventional cycle, the optimal net work, thermal efficiency, and exergy efficiency all increased by 4.87%, 3.62%, and 10.06%, respectively.
[4] Wu et.al. The exhaust gas temperature Tgi (250-500 0C) at the input of the gas heater demonstrates that the unique kind of CDTPC may enhance the net power production by 3.9-26.3% and lower the optimal operating pressure by 13.2-31.0% when compared to the ORC (organic Rankine cycle) and the steam Rankine cycle. Waste heat can be used more efficiently by the double-stage CDTPC when the exhaust gas is not corrosive and by the three-stage CDTPC when the exhaust gas is not corrosive and the temperature is between 412 0C and 500 0C. However, the single-stage CDTPC and the double-stage CDTPC are more efficient at using waste heat when the exhaust gas is corrosive (250 0C Tgi 338 0C and 338 0C Tgi 500 0C, respectively).
[5] Li et.al. presents On the power output and thermal efficiency of the cycles, thermodynamic comparisons of the supercritical SRC, transcritical Rankine cycle, and supercritical or transcritical Rankine cycle with ejector (ESRC, ETRC) are made. According to the results, the cycles' net power production could be sorted from high to low as follows: ESRC > ETRC > SRC > TRC, and the cycles' thermal efficiency could be rated similarly: TRC > SRC > ESRC > ETRC.
[6] Hu et.al. presents The optimal circulation ratio for the ammonia-water power cycle (AWPC), which is based on the Kalina cycle, is 4, with a 12%–13% concentration difference in the ammonia-water solution. Also, increasing the ammonia-water solution concentration will enhance the performance of the AWPC, while increasing the solution heat exchanger's terminal temperature

difference would enhance the ratio of power generation.

[7]Yari et.al. The top cycle is an ejector-expansion transcritical cycle, whereas the bottom cycle is a sub-critical CO2 cycle. The second-law efficiencies decline as the evaporator and/or gas cooler output temperatures rise.

[8] Xia et.al. presents A promising technique for utilising both low and high temperature heat sources is the transcritical carbon dioxide (CO2) cycle. For the low temperature transcritical power cycle, CO2/R32 exhibits the maximum exergy efficiency of 52.85% and the lowest levelized cost per unit of exergy product of 47.909$/MWh among the CO2-based mixtures and pure CO2. CO2/Propane offers the lower levelized cost per unit of energy product for the high temperature transcritical power cycle, at 29.212$/MWh.

[9] Wang et.al.compares the revolutionary single-pressure multi-stage CDTPCs (carbon dioxide transcritical power cycles) and the single-pressure single-stage CDTPC for engine waste heat recovery from a thermodynamic and exergoeconomic perspective. demonstrates that at an exhaust gas temperature of 470 0C, the double-stage CDTPC can generate the greatest net power output of 517.27 kW for a 2928 kW engine.

[10] Sahu et.al. Both the combined refrigeration-power cycle and the transcritical CO2 refrigeration cycle have been researched recently. Under all operating conditions, it has been discovered that the combined power cycle's COP and second-law efficiency are much higher than those of the straightforward cooling-refrigeration cycle. COP rises monotonically with turbine inlet temperature over time. Exergetic efficiency, however, first rises and then falls.

[11] Wang et.al. presents For a variety of applications, different carbon dioxide (CO2) power cycles have been proposed. For high-temperature heat sources, the CO2 power system is more effective than the Rankine cycle of ultra-supercritical steam.

[12] He et.al. describes a desalination system that uses a transcritical carbon dioxide (CO2) Rankine cycle to power the steam compressor (CRC). It has been demonstrated that it is possible to create freshwater using a combined desalination system. Peak values of the net power, Wnet= 64.96 kW, and the corresponding thermal efficiency, CO2= 5.84%, for the CO2 cycle are seen within the examined range of the turbine inlet pressure and temperature. The maximal freshwater production for the MVC subsystem is 1.29 kilogrammes per square metre, and the gained output ratio (GOR) is 2.42. The MVC desalination system will function more effectively if the top temperature is raised, the ambient temperature is lowered, and the TTD of the MVC heater is increased.

[13] Liu et.al. presents utilising both conventional and cutting-edge exergy analysis, a revolutionary two-stage transcritical compressed carbon dioxide energy storage device. The biggest exergy destruction rate of 256.71 kW, accounting for 19.23% of the total exergy destruction rate, designates cold storage as the most important component for improvement. The system's energy efficiency is 59% for the actual cycle, while it is 77.8% at its highest possible level for the inevitable cycle.

[14] Ma.et.al. presents a summary of refrigeration and heat pumps using transcritical carbon dioxide. The performance of the carbon dioxide transcritical process can be raised to a level that is comparable to that of a typical heat pump system by using an internal heat exchanger, two-stage compression, expansion work recovery, and improved heat transfer.

[15] Dzido et.al. presents The most effective use of this technology was found when the CO2 pressure was maximised. Liquid air energy storage technology and transcritical CO2 cycle were combined to increase its efficiency. In a parallel system, efficiency levels are 5-6%, but in a subsequent cycle, they are only 3.5-5%. Due to the temperature cross in this system, heat from the compression part cannot be used to heat the air in the expansion section. Whereas in the parallel mode any pressure increase above 300 bars led to insignificant additional efficiency, pressure increases in the CO2 cycle resulted to a gain in storage efficiency in each case.

[16] Wu et.al. presents the better potential for turning middle-grade waste heat into meaningful work of ORC andCDCPC. Exhaust gas temperature Tgi (250-500 0C) at the gas heater's inlet demonstrates that the novel type of CDTPC can increase net power output by 3.9-26.3% and decrease the optimum working pressure by 13.2-31.0%. The single-stage CDTPC, P4op of the double stage, and three-stage CDTPC can all decrease by 13.2-19.3%, 23.5-31.0%, and Wnet can both increase by 7.3-23. The double-stage CDTPC at 250 0C Tgi 412 0C and the three-stage CDTPC at 412 0C Tgi 500 0C may both use waste heat more efficiently if the exhaust gas is not corrosive. If corrosive exhaust gas is present,Waste heat utilisation is more efficient in the single-stage CDTPC when the temperature is between 250°C and 338°C and in the double-stage CDTPC when the temperature is between 338° 0C and 500° 0C.

[17] Huang et.al. presents an experimental CTPC system is an appropriate engine waste heat recovery (E-WHR) technology, axial turbine expander with conventional carbon ring mechanical seal and angular contact ceramic ball bearings ismanufactured specifically and experimental tests of the turbine expander are conducted on the CTPC test bench. With modifications to the resistance load, the turbine's rotational speed varies from 10,554 rpm to 14,684 rpm, and its maximum power output of 692W is achieved at 14,022 rpm. At 13,366 rpm, maximum efficiency of 53.43% is reached before speeding down. The leakage brought on by the dynamic seal's failure is the cause of the turbine expander's low power output.

[18] Ahmadi et.al. presents a thermodynamic investigation on flat plate collector-based transcritical power cycles on a modest scale. The increase in heat exchanger surface area is brought on by the rise in turbine inlet temperature. The transcritical CO2 power cycle powered by solar energy can operate steadily and continuously throughout the whole of the day. The net power production and system efficiency are less sensitive to changes in the turbine's input temperature. The surface area of heat exchangers increases as the temperature at the turbine inlet rises. The plant's overall investment has been reduced while the system's overall efficiency and solar fraction have both been maximised. An overall thermal efficiency of 10.55% might be attained under best-optimized conditions.

[19] Ge et.al. shows a plate recuperator, an air-cooled finned-tube CO2 condenser, and a CO2 liquid pump. Higher CO2 mass flow rates resulted in higher CO2 pressures at the turbine intake and outlet as well as higher turbine power output. The CO2 mass flow rate was directly governed by the CO2 liquid pump speed. The overall turbine efficiency is lower than the turbine's isentropic efficiency. The highest system thermal efficiency is attained when the system operates at low temperature and high pressure at the turbine inlet.

[20] Li et.al. presents The CTPC systems behave as a second-order underdamped system with the perturbations of pump speed and expansion valve opening; CTPC

systems respond slowly with the perturbations of engine conditions, i.e. pump speed and expansion valve opening, but possess the ability to produce power and operate continuously and safely for few times. Carbon dioxide transcritical power cycle (CTPC) systems are dynamically tested on a constructed test bench using an expansion valve.The CTPC systems exhibit considerable potential for recovering waste heat from truck engines since they are resilient to narrow variations of heat sources and quick to make adjustments when necessary.

[21] Li et.al. presents The comparison of two cycles, the CO2 transcritical power cycle and the ORC, using various working fluids R123, R245fa, R600a, and R601 shows that the ORC performs better thermodynamically and is more successful at recovering low grade heat. The regenerative ORC utilising R601 has the highest thermal (14.05%) and energy efficiency, while the ORC using R123fa generates the most net power (192.7 KW). Economically, the CDTPC outperforms the ORC in terms of net power output.

[22] Shu et.al. presents to look into TRC performance enhancements for the WHR of the engine using CO2 mixes. The range of condensation temperatures for transcritical CO2 combinations can be expanded by the CO2 mixtures. For the TRC with CO2/R161 (0.45/0.55) and CO2/R32 (0.3/0.7) compared to the CTRC, the optimal operation pressure will decrease by 36% and 35%, respectively. The carbon dioxide TRC's net output power increases by 8.8% compared to the CTRC. In comparison to CO2/R32(0.3/0.7), CO2/R32(0.7/0.3) will result in a 29.4% reduction in the ideal total heat transfer area increment.

[23] Meng et.al. presents The compression heat recovery storage system, which was built as part of a solar carbon dioxide transcritical Rankine cycle integration with compressed air energy storage, improves the CO2 Rankine cycle's performance in terms of net power production, thermal efficiency, and exergy efficiency. The negative impact on the pump is lessened in Rankine cycle performance under conditions like high mass flow rate and high air storage pressure thanks to compression heat recovery. The net power production reduces as pump power increases.

[24]Chen et.al. compares the efficiency of an ORC that uses R123 as the working fluid to a CO2 transcritical power cycle that uses energy from low-grade waste heat to generate meaningful work. Transcritical carbon dioxide power systems produce somewhat more power than organic rankine cycles when using low-grade waste heat at the same thermodynamic mean heat rejection temperature.

[25]Baheta et.al. shows the CO2 cycle performance; at 10 MPa gas cooler pressure, the greatest COP was 3.24. Additionally, it was found that the cycle is better suited for air conditioning applications than refrigeration applications since COP rises as evaporator temperature rises.

[26]Garcia et.al. analyses several designs for improving performance, including those with an internal heat exchanger, an ejector, and a turbine. Using an ejector, a turbine, or an internal exchanger, the COP is increased by 35.85%, 24.21%, and 25.74%, respectively, depending on the evaporation method.

2. System Description:

The ambient air at state 1, after being cooled in the mechanical chiller up to state 2 enters the compressors. The compressor compressed the air; resulting at state 3 the Pressure &Temperature of the air is increased. This high Pressure &Temperature air enters in the combustion chamber (CC) where the combustion of the fuel take place. Due to combustion of fuel the flue gases are formed. This flue

gases having high Pressure &Temperature expand in High pressure turbine(HTb) state 4 and expanded gases leaving at 5 are sent to reheat combustion chamber(RCC) for being further heated ,the fluid leaves at state 6 and enters low pressure turbine (LTb)resulting shaft work is found. After expanding the flue gases in turbine, it discharge from turbine and the resulting CO2 is stocked in stock chamber state 8.Asthe CO2 gases stocked, the ammonia-water vapor fluid expand in Ammonia Water Turbine from high pressure drum (state 9). As the CO2 gases stocked, the ammonia-water vapor fluid expand in Ammonia Water Turbine from high pressure drum (state 9).Resulting shaft work is obtained.After expanding it discharge in High pressure Ammonia – Water turbine(HAWT) (state 9-10) and passes from mixer(state 10-11)and then passes through low pressure Ammonia-Water turbine(LAWT) after expanding in this turbine pressure gets decreases and temperature increases (state 11-12),After expanding it discharge in Reheat Heat Exchanger at state 12, where the Pressure &Temperature of the Ammonia Water is decreased as compare state 11. After discharging from RHE from state 12 to state 13 Pressure &Temperature is increased. And then it passed through absorber 13to 14.The absorber absorbs the unwanted gases let as NOx, CO, etc. With the help pump (P2), the Ammonia-Water pumped in a heat exchanger from 14to 15.In heat exchanger the Pressure &Temperature is increased of the Ammonia-Water (15 to 16).The separator (S) separates the rich and lean mixture (16 to 17).The rich mixture enters in feed heater where Pressure &Temperature is increased (state 17 to 18).After it, it enters in condenser at state 18. In condenser (a) indicates cooling water in and (b) indicate hot water out.The vapor form of ammonia-water is converted then to liquid form.With the help of pump (P1) the liquefied Ammonia-Water pumped in feed heater state 20 to 21.The feed heater raises the Pressure &Temperature of liquefied Ammonia-Water and it change in saturated liquid form (state 20 to 21).After passing Feed Heater the saturated liquefied Ammonia-Water enters in heat recovery steam generator (HRSG) where it changes its phase in vapor form and passes through medium pressure drum(MPD) to high pressure drum (HPD)state 21-22-23-24-25,after getting high pressure passes through CO2 turbine (state 25-26) ,the temperature and Pressure of discharge CO2 is increased .And then it discharge in RHE, where Pressure &Temperature is decreased of CO2 due to heat exchange between ambient air and CO2 (state 27 to 28).And then it enters in condenser where the vapor form of CO2 is changed in liquid form of CO2. In condenser state (a) indicates cooling water in and state (b) indicates heat water out. After condensing of CO2the condensate extraction pump (CEP) pumped the CO2liquid in pump (P4) when it change in saturated liquid form. With the help of pump (P3) it pumped in RHVG where it change in vapor form (state 31 to 32) in low pressure drum. Then enters in heat exchanger, Pressure &Temperature is decreased of CO2(state 33 to 34) and then it passed in a throttle device Where a high pressure drop is take place. Resulting the enthalpy of Ammonia-Water vapor is decreased (state 34 to 35) and then it enters again in absorber. In absorber there is heat exchange take place between state35to13 Ammonia -water (thus the process again starts from 1.

3. Thermodynamic Modeling:

The governing equations for various thermodynamic components of the combined cycle power plant under consideration are as follows:

3.1 Gas Model:

Ambient air entering the refrigeration heat exchanger of the low pressure turbine of bottoming cycle of combined cycle power plant is assumed to be at 1.01325 bar. Natural gas is taken to be fuel for the proposed combined cycle [29] with specific heat of combustion gases, given by

$$c_p = a + bT + cT^2 + \ dT^3 + \ \ldots\ldots\ldots\ldots\ldots \quad (1)$$

Where a,b,c,d, etc. are the coefficients of polynomial with their values taken from the work of Toulounkain and Tadash [30]. With the use of equation (1) enthalpy of gas can be calculated as

$$h = \ \int_{T_a}^{T} c_p\,(T)dT \quad (2)$$

All non-reacting gases are arbitrarily assigned zero thermodynamic enthalpy, entropy and availability at the ambient pressure of 1.01325 bar.

3.2 Compressor Model:

An axial flow compressor is used in the considered power plant and inefficiencies are taken care through the concept of polytrophic efficiency [31], by using following expression

$$\frac{dT}{T} = \left[\frac{R}{\eta_{pc}.c_{pa}}\right]\frac{dp}{p} \quad (3)$$

and the corresponding work required by both the compressors is given by:

$$W_c = \left[\dot{m}_a\left(h_{a,i} - h_{a,e}\right)\right]_{lp,c} + \left[\dot{m}_a\left(h_{a,i} - h_{a,e}\right)\right]_{hp,c} \quad (4)$$

Compressor work is estimated as under,

$$W_c = \dot{m}_a[h_{c,e} - h_{c,i}] \quad (5)$$

3.3 Combustion Chamber Model:

In the considered combined cycle the preheating of fuel is considered. Irreversibility in the combustion chamber [32] is taken care by combustion efficiency. It is proposed to preheat the fuel of combustion chamber and fuel of reheat combustion chamber by the coolant which is being discharged from low pressure gas turbine. Value of specific heat of natural gas is taken form works of J.M.Campbell [33].

Mass and energy balance across combustion chamber and reheat combustion chamber for a given turbine inlet temperature provide the fuel required in combustion chamber/reheat combustion chamber

$$\dot{m}_{cc,e} = \ \left[\dot{m}_i + \ \dot{m}_f\right] \quad (6)$$

$$\dot{m}_f.\left(LHV.\eta_{cc} + \Delta T_f.c_{pf}\right) = \ \left[\dot{m}_{cc,e}.h_{cc,e} - \dot{m}_i.h_{cc,i}\right] \quad (7)$$

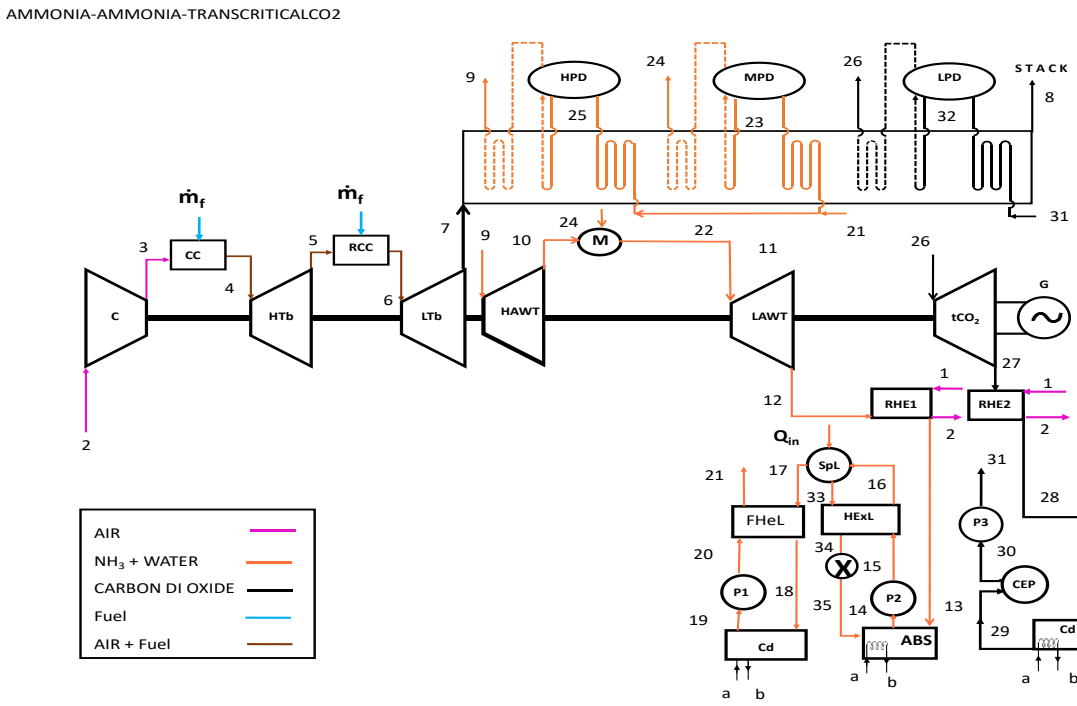

Fig.1 Schematic of combined cycle using ammonia-water mixture and trans critical carbon dioxide

The expansion process is assumed to be polytropic and the temperature at any stage in the turbine is given by

$$\frac{dT_{fg}}{T_{fg}} = \left[\frac{p+dp}{p}\right]^{\frac{R.\eta_{pgt}}{c_{pa}}} - 1 \quad (8)$$

And the corresponding gas turbine work is given by

$$W_{gt} = \left[m_{fg,i}\left(h_{fg,i} - h_{fg,e}\right) + \sum \dot{m}_{coolant}.\left(h_{coolant,e} - h_{coolant,i}\right)\right]_{hpgt} + \left[m_{fg,i}\left(h_{fg,i} - h_{fg,e}\right) + \sum \dot{m}_{coolant}.\left(h_{coolant,e} - h_{coolant,i}\right)\right]_{lpgt} \quad (9)$$

Calculation of enthalpy of ammonia water mixture is defined in Appendix-A

3.4 Transcritical carbondioxide/Ammonia Water mixture turbine Model:

Here it is assumed that the dissociation of ammonia does not take place in the binary mixture. Considering the isentropic efficiency of transcritical carbon dioxide turbine and ammonia-water mixture turbine, the gross turbine work output is given by the following equation

$$W_{st} = \left[\dot{m}_{s,hp}.\eta_{ishp}.\left(h_{s,i} - h_{s,e}\right)\right] + \left[\dot{m}_{s,lp}\eta_{islp}\left(h_{s,i} - h_{s,e}\right)\right] + \left[\dot{m}_{amw,hp}\eta_{islp}\left(h_{amw,i} - h_{amw,e}\right)\right] \quad (10)$$

3.5 Condenser Model:

The condenser of the combined cycle power plant is externally water cooled condenser and shared by intermediate transcritical carbon dioxide turbine and low pressure turbine. Mass and energy balance as given below gives the mass flow required for cooling purpose.

$$\dot{m}_{cw}(\dot{h}_{cw,e} - \dot{h}_{cw,i}) = \dot{m}_{s,lp}.\left(h_{s,i} - h_{water,e}\right) + \dot{m}_{amw,lp}.\left(h_{amw,i} - h_{amw,e}\right) \quad (11)$$

3.6 Pump model:

Pump efficiency is introduced to take care of all the inefficiency of the pump.

$$w_{pump,actual} = \frac{w_{is,pump}}{\eta_{is,pump}} \quad (12)$$

3.7 Performance Parameters:

Performance parameters of the considered combined cycle power plant are as follows:

$$W_{gt,net} = W_{gt} - \frac{W_c}{\eta_M} \quad (13)$$

$$W_{AWT/tCO2} = W_{st}.\eta_{M,st} - \frac{W_p}{\eta_p} \quad (14)$$

$$W_{combined\ cycle} = \left[W_{gt,net} + W_{AWT/tCO2}\right].\eta_{gen.} \quad (15)$$

$$\eta_{I,combined\ cycle} = \frac{W_{combined\ cycle} + \frac{Q_{cool}}{\eta_{II,ref}}}{\dot{m_f}.CV + Q} \quad (16)$$

Where $Q_{cool} = \dot{m}[h_{amw,in} - h_{amw,out} - T_o(s_{amw,in} - s_{amw,out})]$

$$COP = \frac{Cooling\ produced}{Potential\ work\ lost}[35] \quad (17)$$

Table 1: Irreversibility and associated cost function of different thermodynamic components

Component	Irreversibility associated with component
Compressor	$\dot{I}_{compressor} = T_o.[\dot{m}_a.(s_e - s_i)]$
Combustion Chamber	$\dot{I}_{cc} = T_o.\left[\dot{m}_{fg}.s_{fg} - \dot{m}_{a,i}.s_{a,i}\right]$
Gas turbine	$\dot{I}_{gt} = T_o.[\dot{m}_{fg}.(s_{fg,i} - s_{fg,e}) + \sum_{stage} \dot{m}_{coolant}.(s_{coolant,e} - s_{coolant,i})]$
Bottoming cycle turbine	$\dot{I}_{tCO2/amwt} = T_o.[\dot{m}_{fg}.(s_{fg,i} - s_{fg,e})]$
Pump	$\dot{I}_{pump} = T_o\left[\dot{m}_{s/amw}(s_o - s_i)\right]$
Condenser	$\dot{I}_{condenser} = T_o\left[\sum_j \dot{m}_j.(s_{j,i} - s_{j,o}) - m_w c_{p,w}\, ln\frac{T_{w/i}}{T_{w/o}}\right]$
Mechanical chiller	$\dot{I}_{M/C} = T_o.[\dot{m}_a.(s_i - s_o)]$
Heat exchanger	$\dot{I}_{HE} = T_o\left[m_{we/sol.}(s_{we/sol.,i} - s_{we/sol.,o}) - m_{w/sol.}(s_{w/sol.,o} - s_{w/sol.,i})\right]$
Refrigerant heat exchanger	$\dot{I}_{RHE} = T_o.\left[\dot{m}_{amw}.(s_{amw,o} - s_{amw,i}) - \dot{m}_{air}.(s_o - s_i)\right]$
Feed heater	$\dot{I}_{FH} = (s_{r/sol.,i} - s_{r/sol.,o}) - (s_{fr/sol.,o} - s_{fr/sol.,i})$
Absorber	$I_{Absorber} = T_o\left[\dot{m}_{wo/sol.}(s_{mix,i} - s_{mix,o}) - m_w c_{p,w}\, ln\frac{T_{w/i}}{T_{w/o}}\right]$
Fuel Compressor	$\dot{I}_{compressor} = T_o.[\dot{m}_f.(s_e - s_i)]$

$$\eta_{II,combined\ cycle} = \frac{W_{combined\ cycle} + Q_{cool}}{\dot{m_f}.G_r}(35)$$

$$\eta_{II,RHE} = \frac{Exergy\ of\ outgoing\ fluids}{Exergy\ of\ incoming\ fluids}[16] \quad (36)$$

Mathematical modeling has been carried out using the equations described above for thermodynamic analysis of the cycle under consideration.

4. Results and Discussion

The work produced, first law efficiency, second law efficiency, and COP are shown to vary with cycle pressure ratio, turbine inlet temperature, ammonia mass fraction, and ambient temperature based on the results of thermodynamic modeling.

With various cycle pressure ratios, turbine inlet temperatures, ammonia mass fractions, and ambient temperatures, Fig. 3 shows the fluctuation in the work generated in the combined cycle. When the ammonia mass fraction is increased, the work produced by the combined cycle decreases because the mixture's specific heat decreases, which lowers the mixture's enthalpy and, in turn, the work produced. This variation is taken into account at an ambient temperature of 30°C while maintaining the same cycle pressure ratio and turbine inlet temperature.

While maintaining the same ammonia mass percentage, more work is produced if the cycles pressure ratio or the turbine inlet temperature are increased.

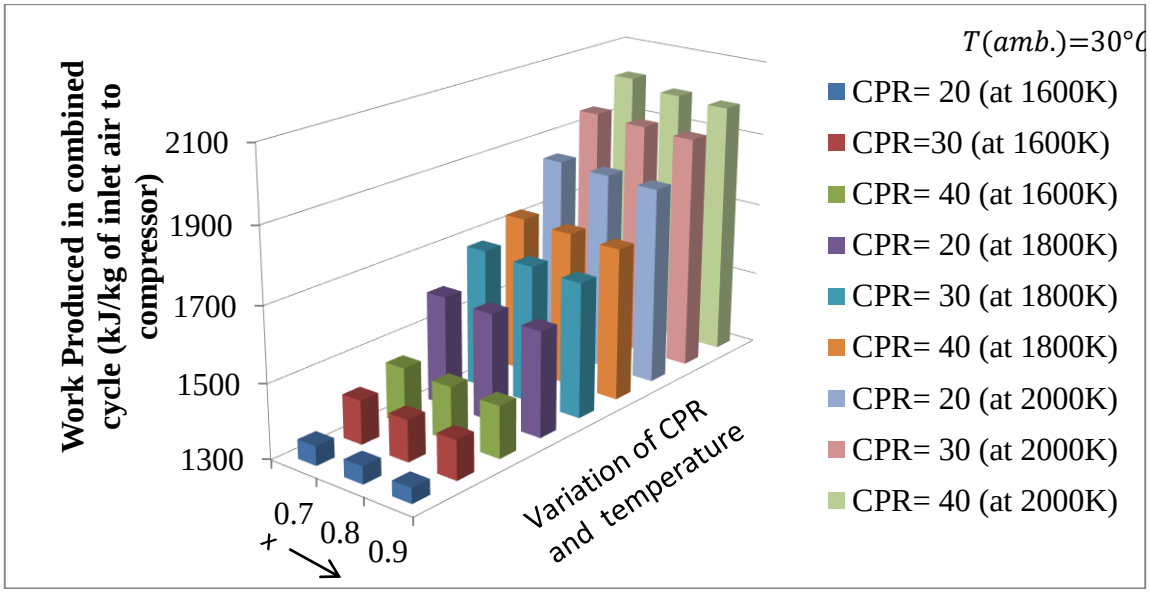

Fig. 3(a) Variation in work produced of the combined cycle with varying cycle pressure ratio, turbine inlet temperature and ammonia mass fraction at ambient temperature of 30°C.

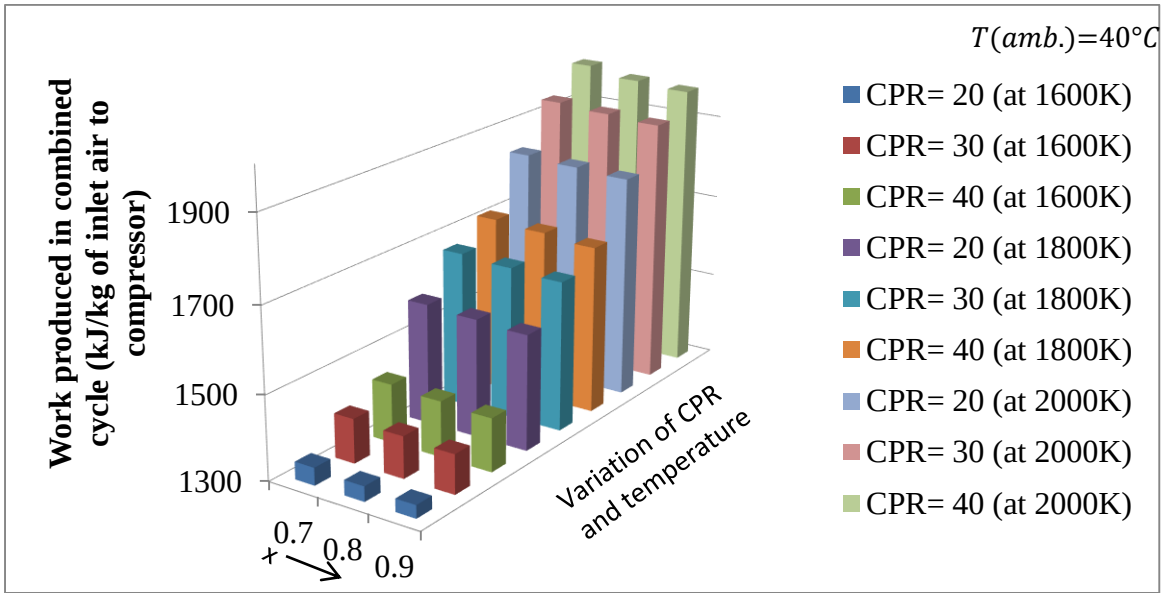

Fig. 3(b) Variation in work produced of the combined cycle with varying cycle pressure ratio, turbine inlet temperature and ammonia mass fraction at ambient temperature of 40°C.

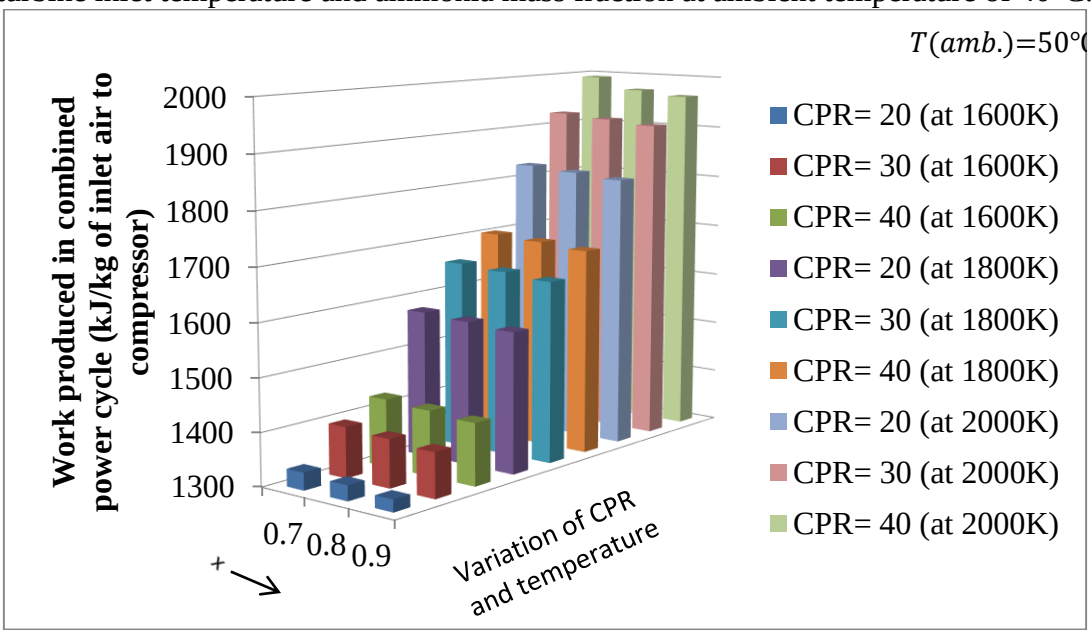

Fig.3(c) Variation in work produced of the combined cycle with varying cycle pressure ratio, turbine inlet temperature and ammonia mass fraction at ambient temperature of 50°C.

The variation with ambient temperature is also shown in Fig. 3. As the ambient temperature rises, less work is produced because the cooling load on the refrigerant heat exchanger increases, which raises the temperature of the fluid entering the compressor and lessens the amount of work the combined cycle can produce.

Figure 4 illustrates how the first law's efficiency varies in relation to the cycle pressure ratio, turbine inlet temperature, ammonia mass percent, and outside temperature. Because the combined cycle's output of work decreases with an increase in ammonia mass percentage, efficiency is seen to decline. While raising the turbine inlet temperature and cycle pressure ratio will boost the cycle's efficiency. The efficiency of the cycle's first law is reduced as a result of a rise in ambient temperature.

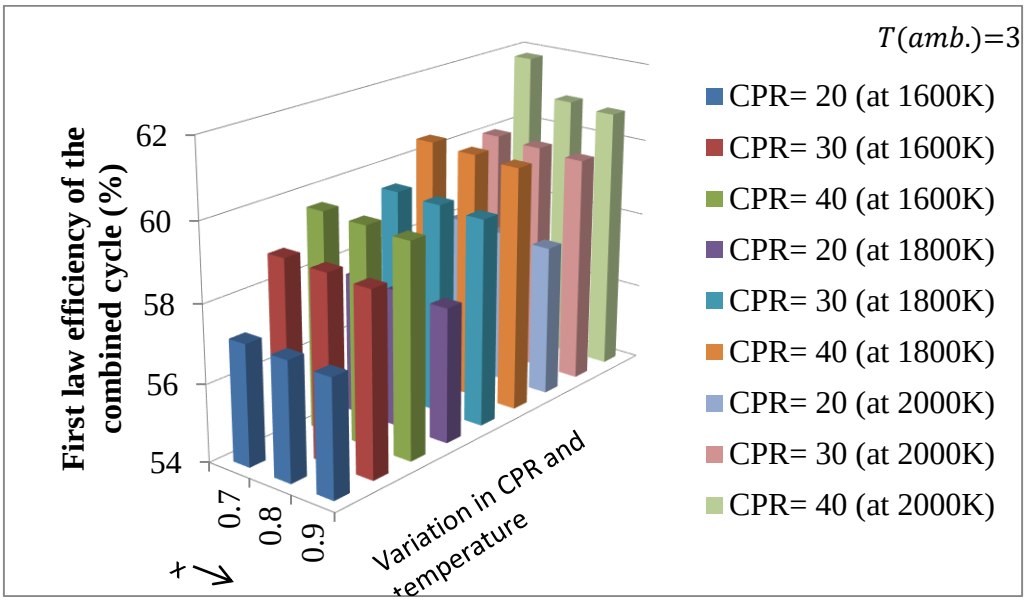

Fig. 4(a) Variation in first law efficiency of the combined cycle with varying cycle pressure ratio, turbine inlet temperature and ammonia mass fraction at ambient temperature of 30°C.

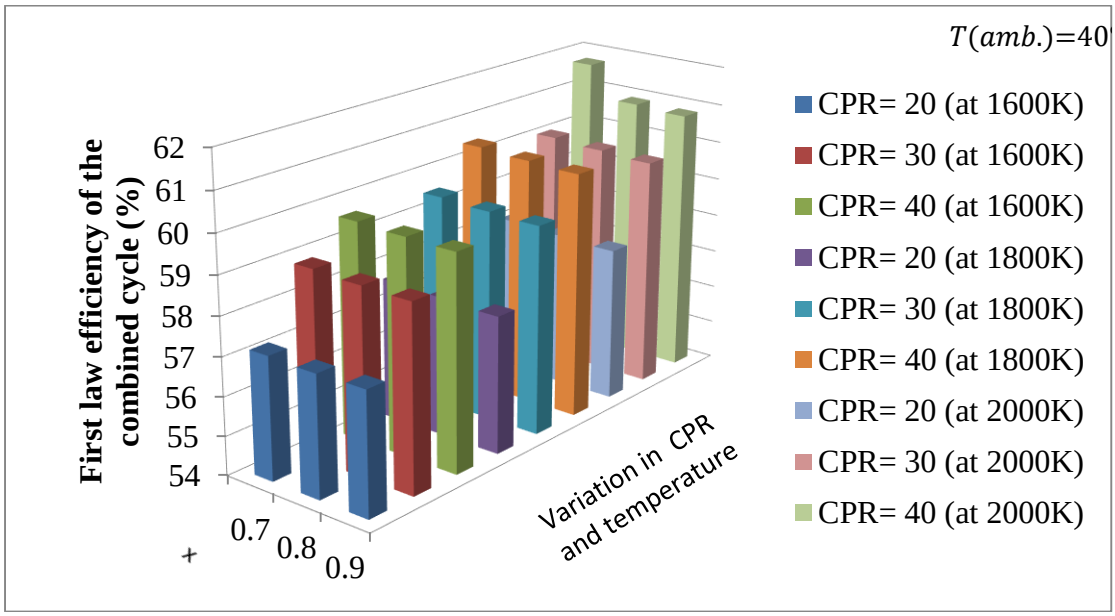

Fig.4 (b) Variation in first law efficiency of the combined cycle with varying cycle pressure ratio, turbine inlet temperature and ammonia mass fraction at ambient temperature of 40°C.

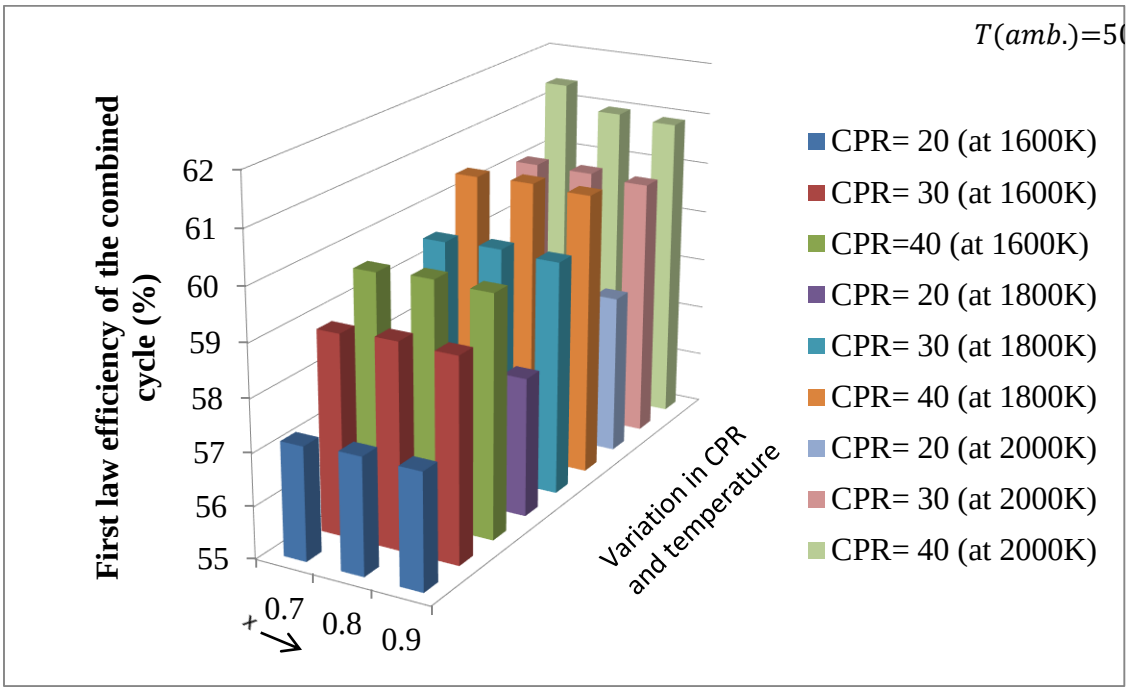

Fig.4(c) Variation in first law efficiency of the combined cycle with varying cycle pressure ratio, turbine inlet temperature and ammonia mass fraction at ambient temperature of 50°C.

Figure 5 shows the combined's variation in second law efficiency. It demonstrates that second law efficiency declines as ambient temperature rises.Furthermore, despite an increase in reported mixture flow velocity, a drop in second law efficiency results from a rise in ammonia mass fraction (while maintaining other parameters constant). Furthermore, the combined cycle's second law efficiency is increased by the effects of the cycle pressure ratio and turbine inlet temperature.

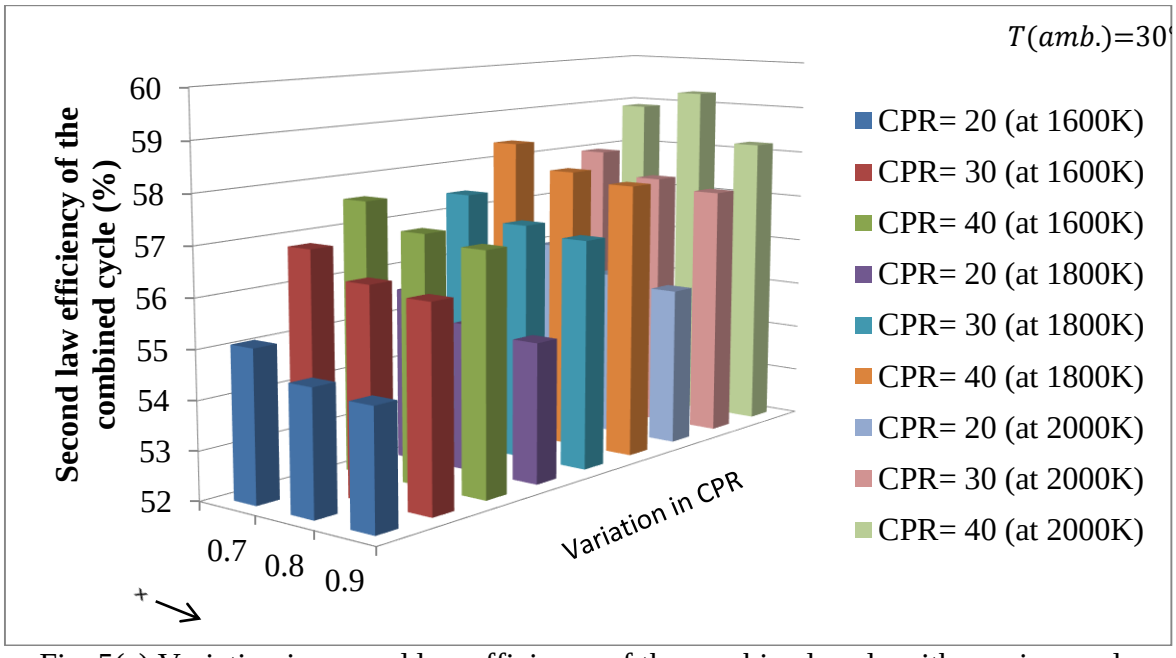

Fig. 5(a) Variation in second law efficiency of the combined cycle with varying cycle pressure ratio, turbine inlet temperature and ammonia mass fraction at ambient temperature of 30°C.

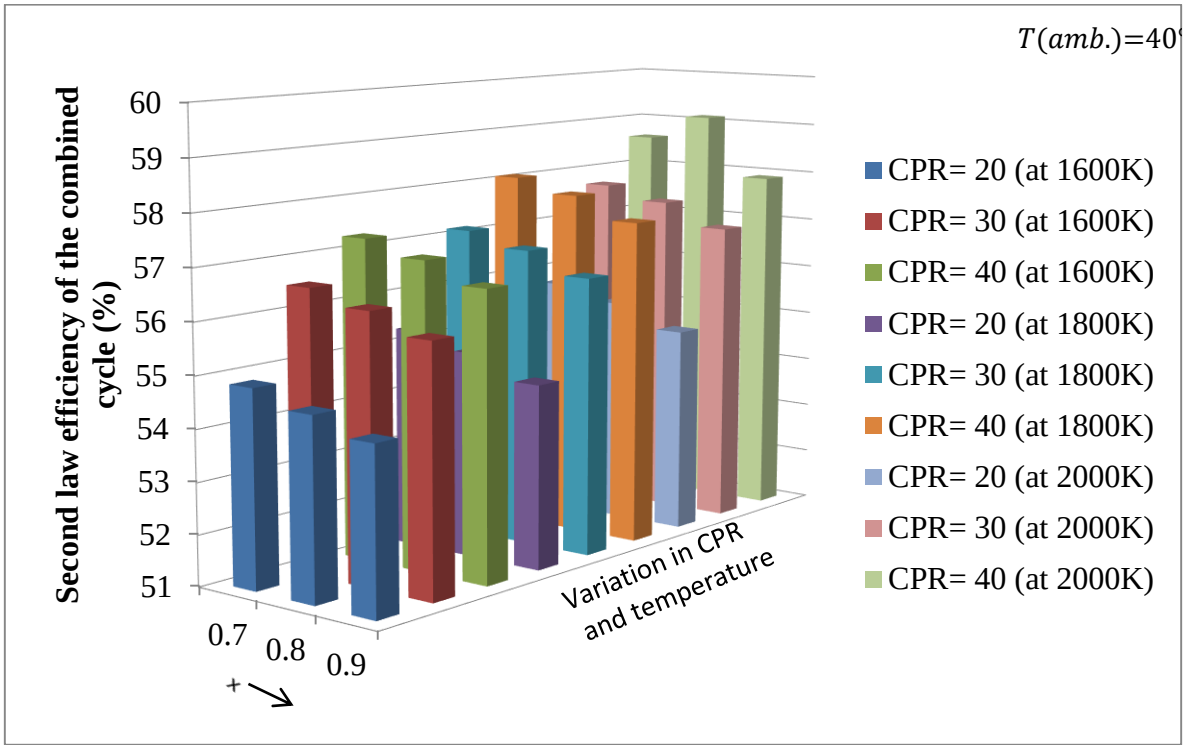

Fig. 5(b) Variation in second law efficiency of the combined cycle with varying cycle pressure ratio, turbine inlet temperature and ammonia mass fraction at ambient temperature of 40°C.

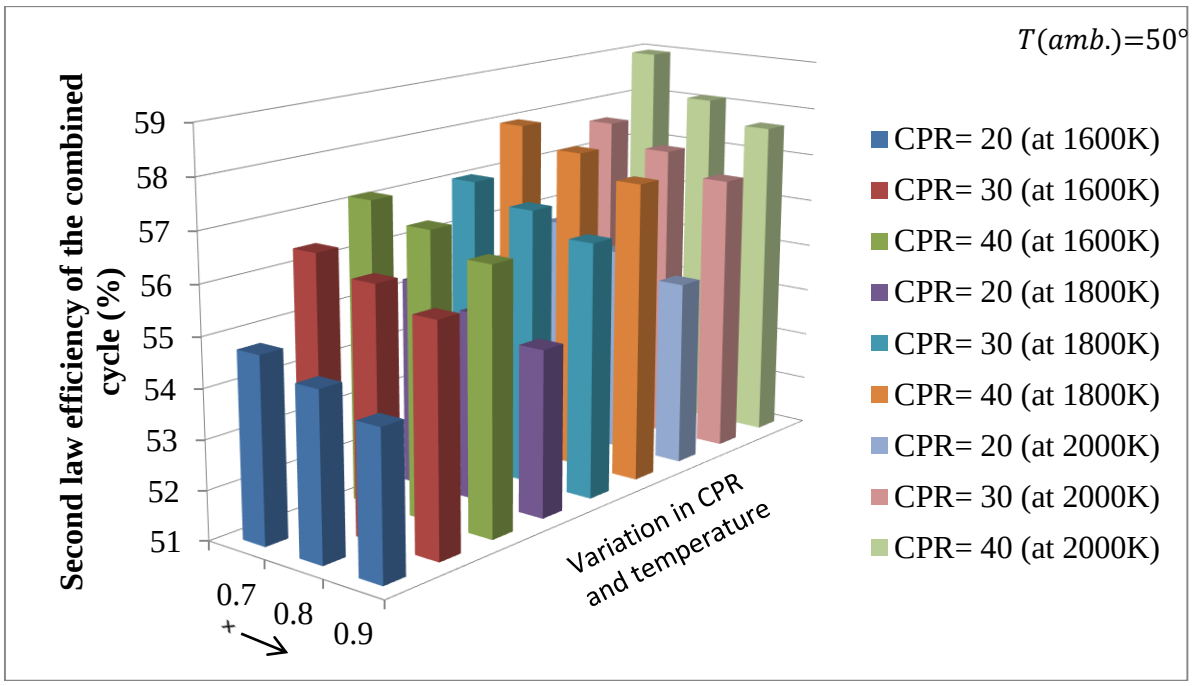

Fig.5(c) Variation in second law efficiency of the combined cycle with varying cycle pressure ratio, turbine inlet temperature and ammonia mass fraction at ambient temperature of 50°C.

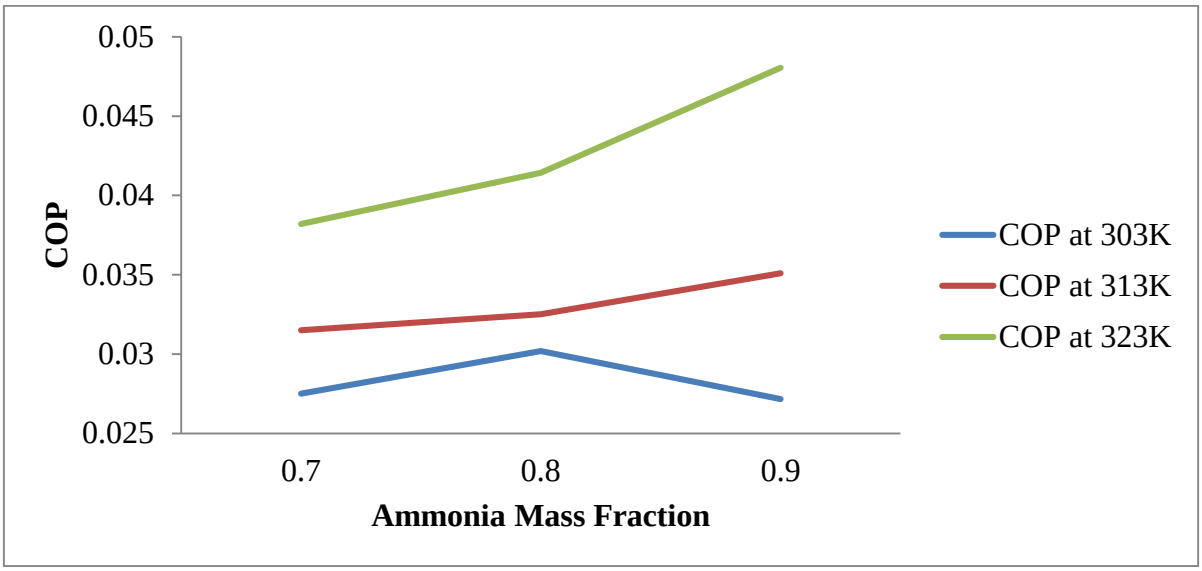

Fig. 6 Variation in coefficient of performance of the cycle with varying ammonia mass fraction.

Modeling of COP demonstrates that it is unaffected by the working fluid's mass flow rate. Furthermore, the low pressure turbine's temperature and pressure variations are limited to a short range (75°C to 100°C and 4 bar, respectively). Here, the COP of the cycle is only examined in relation to the mass fraction of ammonia and the surrounding environment.

Figure 6 illustrates how COP changes when the ammonia mass percentage and ambient conditions change. According to the graphical representation, the cycle's COP will rise as ambient air temperature rises for constant ammonia mass fraction due to an increase in cooling demand.With an increase in ammonia mass percentage, the potential work loss and the cooling load both decrease for constant ambient air temperature, but the work loss is greater than the cooling load, leading to the observation of a decline in COP.At 30°C and at an ammonia mass fraction of 0.8, an ambiguity in the COP is seen, and the COP then starts to decline.

Conclusions:

Following conclusions are drawn from the present study:

- Maximum work output and combined cycle efficiency are noted for cycle pressure ratios of 40, 2000 K turbine inlet temperature, 0.7 ammonia mass fraction, and 30 C ambient temperature. Efficiency was measured to be 2035kJ/kg and work was observed to be 62.01% .
- For the first law condition mentioned above, the combined cycle's second law efficiency is found to be 60.27%.
- At 303K, the coefficient of performance exhibits an interesting pattern, increasing from 0.7 to 0.8 of the ammonia mass fraction before declining beyond 0.8.

APPENDIX - A

A mixture if used as a working fluid offers varying boiling temperature and condensation temperature. For binary mixture (like mixture of ammonia water) following equation developed by J.PatekandJ.Klomfar [36]are used for calculating the boiling point and condensing point (also referred as bubble point and dew point)

$$T_b(p,x) = T_0 \sum_i a_i (1-x)^{m_i} \left[ln(\frac{p_0}{p}) \right]^{n_i} \quad (A.1)$$

$$T_d(p,y) = T_0 \sum_i a_i (1-y)^{\frac{m_i}{4}} \left[ln(\frac{p_0}{p})\right]^{n_i} \quad (A.2)$$

If binary mixture exist in equilibrium then the amount of vapor that is in equilibrium with the vapor phase at a given pressure is given by the works of G.SoleimaniAlamdari [37]

$$y = 1 - exp\left[ap^b x + \left(c + \frac{d}{p}\right)x^2\right] \quad (A.3)$$

The Gibbs free energy at any state is given by [38]

For liquid phase:

$$g_R^l = (1-x)g_{H_2O,R}^l + xg_{NH_3,R}^l + RT(1-x)\ln(1-x) + xlnx + g_{E,R} \quad (A.4)$$

For gas phase:

$$g_R^g = (1-y)g_{H_2O,R}^g + yg_{NH_3,R}^g + RT(1-y)\ln(1-y) + yln \quad (A.5)$$

And on the basis of Gibbs free energy enthalpy and entropy of the binary mixture can be evaluated as follows

$$h = -RT_B T_R^2 \left[\frac{\partial}{\partial T_R}\left(g_R/T_R\right)\right]_{p_R} \quad (A.6)$$

$$s = -R\left[\frac{\partial g_R}{\partial T_R}\right]_{P_R} \quad (A.7)$$

The excess specific enthalpy and specific entropy for the liquid mixture isgiven by:

$$h^E = -RT_B T_R^2 \left[\frac{\partial}{\partial T_R}\left(g_R^E/T_R\right)\right]_{p_{R,x}} \quad (A.8)$$

$$s^E = -R\left[\frac{\partial g_R^E}{\partial T_R}\right]_{P_{R,x}} \quad (A.9)$$

Therefore the specific enthalpy, entropy for the liquid mixture are given by

$$h_m^l = xh_{NH_3}^l + (1-x)h_{H_2O}^l + h^E \quad (A.10)$$

$$s_m^l = xs_{NH_3}^l + (1-x)s_{H_2O}^l + s^E + s^{mix} \quad (A.11)$$

5. References

1. Chen, Yang, and Per Lundqvist. "The CO2 transcritical power cycle for low grade heat recovery: Discussion on temperature profiles in system heat exchangers." ASME Power Conference. Vol. 44595. 2011.
2. Aqel, Omar A., et al. "Sensitivity of transcritical cycle and turbine design to dopant fraction in CO2-based working fluids." Applied Thermal Engineering 190 (2021): 116796.
3. Wang, Z. X., et al. "Parameter analysis of an ammonia-water power cycle with a gravity assisted thermal driven “pump” for low-grade heat recovery." Renewable Energy 146 (2020): 651-661.
4. Wu, Chuang, et al. "System optimisation and performance analysis of CO2 transcritical power cycle for waste heat recovery." Energy 100 (2016): 391-400.
5. Li, Xinguo, Haijun Huang, and Wenjing Zhao. "A supercritical or transcritical Rankine cycle with ejector using low-grade heat." Energy conversion and management 78 (2014): 551-558.
6. Hu, Bing, et al. "Thermodynamic analysis of a new ammonia-water power cycle." Energy Reports 6 (2020): 567-573.
7. Yari, Mortaza, and S. M. S. Mahmoudi. "Thermodynamic analysis and optimization of novel ejector-expansion TRCC (transcritical CO2) cascade refrigeration cycles (Novel transcritical CO2

cycle)." Energy 36.12 (2011): 6839-6850.
8. Xia, Jiaxi, et al. "Thermo-economic analysis and comparative study of transcritical power cycles using CO2-based mixtures as working fluids." Applied Thermal Engineering 144 (2018): 31-44.
9. Wang, Shun-sen, Chuang Wu, and Jun Li. "Exergoeconomic analysis and optimization of single-pressure single-stage and multi-stage CO2 transcritical power cycles for engine waste heat recovery: A comparative study." Energy 142 (2018): 559-577.
10. Sahu, Anjan Kumar, Neeraj Agrawal, and Prasant Nanda. "A parametric study of transcritical CO2 simple cooling cycle and combined power cycle." International Journal of Low-Carbon Technologies 12.4 (2017): 383-391.
11. Wang, Zhe, et al. "A partial heating supercritical CO2 nested transcritical CO2 cascade power cycle for marine engine waste heat recovery: Thermodynamic, economic, and footprint analysis." Energy 261 (2022): 125269.
12. He, W. F., et al. "A mechanical vapor compression desalination system coupled with a transcritical carbon dioxide Rankine cycle." Desalination 425 (2018): 1-11.
13. Liu, Zhan, et al. "Conventional and advanced exergy analysis of a novel transcritical compressed carbon dioxide energy storage system." Energy conversion and management 198 (2019): 111807.
14. Ma, Yitai, Zhongyan Liu, and Hua Tian. "A review of transcritical carbon dioxide heat pump and refrigeration cycles." Energy 55 (2013): 156-172.
15. Dzido, Aleksandra, Marcin Wołowicz, and Piotr Krawczyk. "Transcritical carbon dioxide cycle as a way to improve the efficiency of a Liquid Air Energy Storage system." Renewable Energy 196 (2022): 1385-1391.
16. Wu, Chuang, et al. "System optimisation and performance analysis of CO2 transcritical power cycle for waste heat recovery." Energy 100 (2016): 391-400.
17. Huang, Guangdai, et al. "Experiments on a small-scale axial turbine expander used in CO2 transcritical power cycle." Applied Energy 255 (2019): 113853.
18. Ahmadi, Mohammad H., et al. "Thermo-economic analysis and multi-objective optimization of a transcritical CO2 power cycle driven by solar energy and LNG cold recovery." Thermal Science and Engineering Progress 4 (2017): 185-196.
19. Ge, Y. T., et al. "Performance evaluation of a low-grade power generation system with CO2 transcritical power cycles." Applied energy 227 (2018): 220-230.
20. Li, Xiaoya, et al. "Effects of external perturbations on dynamic performance of carbon dioxide transcritical power cycles for truck engine waste heat recovery." Energy 163 (2018): 920-931.
21. Li, Maoqing, et al. "Thermo-economic analysis and comparison of a CO2 transcritical power cycle and an organic Rankine cycle." Geothermics 50 (2014): 101-111.
22. Shu, Gequn, et al. "Potential of the transcritical Rankine cycle using CO2-based binary zeotropic mixtures for engine's waste heat recovery." Energy Conversion and Management 174 (2018): 668-685.
23. Meng, Fanxiao, et al. "Thermo-economic analysis of transcritical

CO2 power cycle and comparison with Kalina cycle and ORC for a low-temperature heat source." Energy Conversion and Management 195 (2019): 1295-1308.
24. Chen, Yang, et al. "A comparative study of the carbon dioxide transcritical power cycle compared with an organic Rankine cycle with R123 as working fluid in waste heat recovery." Applied thermal engineering 26.17-18 (2006): 2142-2147.
25. Baheta, AkliluTesfamichael, et al. "Performance investigation of transcritical carbon dioxide refrigeration cycle." Procedia Cirp 26 (2015): 482-485.
26. Pérez-García, V., et al. "Comparative analysis of energy improvements in single transcritical cycle in refrigeration mode." Applied Thermal Engineering 99 (2016): 866-872.

Nomenclature Used:

Symbol	**Specification (Unit)**
c_p	Specific heat at constant pressure (kJ/kg.K)
R	Universal Gas constant (kJ/kg.K)
p	Pressure (bar)
h	Enthalpy (kJ/kg)
T	Temperature (K)
$\dot{m}$	Mass flow rate (kg/second)
LHV	Lower heating value (kJ/kg)
CPR	Cycle Pressure ratio
a,b,c,d,T_o,m_i,p_o,T_B	Constants
W	Work (kJ/kg or kJ/kg of inlet air)
bd	Blow down loss
Q	Refrigerating effect/Heat Input
x	Mass Fraction of ammonia in liquid phase
y	Mass Fraction of ammonia in vapor phase
g	Gibbs free Energy

Abbreviations Used:

HD	High Pressure Drum
ID	Intermediate Pressure Drum
LD	Low Pressure Drum
HRVG	Heat Recovery Vapor Generator

Greek Symbols:

η	Efficiency
$\boldsymbol{\varepsilon}$	Effectiveness

Superscripts:

L	Liquid
G	Gas
E	Excess

Subscripts:

Symbol	Specification
p	Polytrophic (if not used with 'c')
a	Air
c	Compressor
e	Exit
i	Inlet
cc	Combustion Chamber
f	Fuel
fg	Flue gas
s	Steam
hp	High pressure
ip	Intermediate pressure
lp	Low pressure
amw	Ammonia Water Mixture
gt	Gas Turbine
st	Steam Turbine
cw	Cooling Water
M	Mechanical
p	Pump
CV	Calorific Value
gen	Generator
is	Isentropic
b	Boiling point
d	Condensing point
R	Reduced
E	Excess
m	Mixture

Details of Parameter, Term, Symbol and Unit considered:

Parameter	Term, Symbol	Unit
Gas Properties	Specific heat, $c_p = f(T)$ Enthalpy, $h = c_p(T)dT$	kJ/kg.K kJ/kg
Compressor	Polytropic efficiency, (η_{pc}) = 92.0 Mechanical Efficiency, (η_M) = 98.5	% %
Combustor	Efficiency of combustion chamber, (η_{cc}) = 99.5 Loss of pressure in combustion chamber , (p_{loss}) = 2% of inlet pressure Lower heating value, (LHV) = 48990	% bar kJ/kg
Gas turbine	Polytropic efficiency, (η_{pgt}) = 92.0 Exhaust pressure = 1.08 Maximum permissible blade temperature of gas turbine = 1123	% bar K
HRVG (Triple Pressure)	Effectiveness = 98.0 Loss in pressure = 10% of entry pressure (for bottoming cycle fluid) Loss of pressure on the gas side = 6% of pressure at inlet Minimum exhaust temperature from HRVG = 353.0 Pressure of steam in the HD = 160	% bar bar K bar

	Maximum temperature attained due to superheating in H.P. = 873 (Max.) Exhaust pressure from high pressure steam turbine= 35 Pressure loss in reheater = 3% of pressure at inlet Intermediate pressure= 35.0 bar Superheating of steam in I.P. = 673.0 (Max.) Inlet pressure of ammonia water mixture cycle = 4.0 L.P Turbine Inlet Temperature= 348 to 373 Pressure at which deaerator is operating = 2.0 Pressure at which condenser is operating = 0.07 Approach temperature difference between gas/steam or gas/ammonia water mixture = 20.0(min.) Pinch point = 20.0 (min.)	K bar bar bar K bar K bar bar K K
Steam Turbine	Isentropic efficiency of 'hp' steam turbine, ($\eta_{is,hp}$) = 88.0 Isentropic efficiency of 'ip' steam turbine, ($\eta_{is,ip}$) = 88.0 Isentropic efficiency of 'lp' turbine, ($\eta_{is,lp}$) = 88.0 Minimum Steam quality at exit to low pressure steam turbine = 0.85	% % %
Ammonia Mass Fraction	0.7-0.9	
Pump	Isentropic efficiency of pump's, (η_{pump}) = 88.0	%
Generator	Efficiency of generator, ($\eta_{gen.}$) = 88.0	%